Title

Kinetics of Amyloid β-Protein Degradation Determined by Novel Fluorescence- and Fluorescence Polarization-based Assays*

Journal

Journal of Biological Chemistry, 278(39)

ISSN

0021-9258

Authors

Stein, Ross L
Leissring, Malcolm A
Lu, Alice
et al.

Publication Date

2003-09-01

DOI

10.1074/jbc.m305627200

Peer reviewed

THE JOURNAL OF BIOLOGICAL CHEMISTRY
Vol. 278, No. 39, Issue of September 26, pp. 37314–37320, 2003
Printed in U.S.A.

Kinetics of Amyloid β-Protein Degradation Determined by Novel Fluorescence- and Fluorescence Polarization-based Assays*

Received for publication, May 29, 2003, and in revised form, July 2, 2003
Published, JBC Papers in Press, July 16, 2003, DOI 10.1074/jbc.M305627200

Malcolm A. Leissring, Alice Lu, Margaret M. Condron, David B. Teplow, Ross L. Stein‡, Wesley Farris, and Dennis J. Selkoe§

From the Center for Neurologic Diseases, Harvard Medical School and, Brigham and Women's Hospital, Boston, Massachusetts 02115 and the ‡Laboratory for Drug Discovery in Neurodegeneration, Harvard Center for Neurodegeneration and Repair, Cambridge, Massachusetts 02135

Proteases that degrade the amyloid β-protein (Aβ) are important regulators of brain Aβ levels in health and in Alzheimer's disease, yet few practical methods exist to study their detailed kinetics. Here, we describe robust and quantitative Aβ degradation assays based on the novel substrate, fluorescein-Aβ-(1–40)-Lys-biotin (FAβB). Liquid chromatography/mass spectrometric analysis shows that FAβB is hydrolyzed at closely similar sites as wild-type Aβ by neprilysin and insulin-degrading enzyme, the two most widely studied Aβ-degrading proteases. The derivatized peptide is an avid substrate and is suitable for use with biological samples and in high throughput compound screening. The assays we have developed are easily implemented and are particularly useful for the generation of quantitative kinetic data, as we demonstrate by determining the kinetic parameters of FAβB degradation by several Aβ-degrading proteases, including plasmin, which has not previously been characterized. The use of these assays should yield additional new insights into the biology of Aβ-degrading proteases and facilitate the identification of activators and inhibitors of such enzymes.

Progressive accumulation of the amyloid β-protein (Aβ)[1] in brain regions important for memory and cognition is a defining pathogenic feature of Alzheimer's disease (AD). Nevertheless, the causes of elevated brain Aβ levels in the vast majority of AD patients remain unknown. With the exception of rare familial forms of the disease, there is little evidence that AD is attributable to the overproduction of Aβ. Instead, failed clearance of the peptide, including defects in its proteolytic degradation, could underlie its accumulation with age, a possibility that is gaining increasing experimental support (1). Significant elevations in cerebral Aβ levels have now been observed *in vivo* in gene-targeted mice lacking each of several Aβ-degrading proteases: neprilysin (NEP) (2), endothelin-converting enzyme-1 and -2 (3), and insulin-degrading enzyme (IDE) (4, 5). Moreover, several genetic studies have reported linkage and/or allelic association between late onset AD and polymorphisms near or within the IDE gene on chromosome 10q (6–8).

Progress in elucidating the mechanisms underlying the production of Aβ from its protein precursor, APP, by the β- and γ-secretases has depended critically on the development of sensitive, reliable, and accessible assays for quantifying Aβ levels in biological samples. More recently, assays for directly measuring the activity of the secretases have been described (9–11), enabling significant progress in the biochemical characterization of these proteases and the identification and characterization of small-molecule inhibitors. In contrast, relatively few techniques and assays for studying Aβ degradation have been reported, and the most commonly used general methods (*e.g.* measurement of radiolabeled peptides by trichloroacetic acid precipitation or HPLC) are cumbersome and ill suited for accurate quantification of kinetic constants or for high throughput assays. To overcome these difficulties, we have developed novel degradation assays based on a derivatized Aβ peptide, fluorescein-Aβ-(1–40)-Lys-biotin (FAβB). This substrate is efficiently degraded by several known Aβ-degrading proteases and shows a similar inhibition profile as wild-type Aβ in biological samples. The assays we describe are sensitive, quantitative, and easily implemented, with one version requiring no specialized equipment other than a fluorometer. In addition, we describe a versatile fluorescence polarization (FP)-based assay that is both highly quantitative and suitable for high throughput compound screening. We use these assays to quantify the kinetics of Aβ degradation by IDE, NEP, and plasmin.

MATERIALS AND METHODS

Aβ Peptides—Fluorescein-Aβ-(1–40)-Lys-biotin and fluorescein-Aβ-(1–28)-biotin were synthesized by New England Peptide, Inc. (Fitchburg, MA). Biotin was attached to the carboxyl-terminal lysine side chain via an aminocaproic linker, and 5(6)-carboxyfluorescein (Sigma catalog no. C7153) was attached to the amino terminus via a peptide bond. Nonderivatized (wild-type) Aβ peptides were synthesized on an automated peptide synthesizer (Applied Biosystems model 433A) by 9-fluorenylmethoxycarbonyl-based methods. In preparation for quantitative kinetic determinations, aggregated species were removed by centrifuging freshly dissolved peptide (~20 to ~150 μM in 50 mM Tris-HCl, pH 7.4) at 100,000 × *g* for 3 h and carefully removing the top two-thirds of the resulting supernatant, which was immediately aliquoted and stored at −80 °C until further use. Peptide concentrations were determined by amino acid analysis.

Amino Acid Analysis—Samples in 50-mm glass tubes were dried *in vacuo* and then transferred to a hydrolysis vessel (Millipore Corp., Marloborough, MA; part no. 007603). Approximately 300 μl of 6 N HCl was added to the vessel, which was then alternatively purged with nitrogen and evacuated three times before being sealed under vacuum. Vapor phase hydrolysis was performed by heating at 110 °C for 22 h. Separation and quantitation of amino acids was carried out on a Beckman model 6300 amino acid analyzer. Each sample was analyzed in triplicate. Absolute peptide concentrations typically ranged from one-

* The costs of publication of this article were defrayed in part by the payment of page charges. This article must therefore be hereby marked "*advertisement*" in accordance with 18 U.S.C. Section 1734 solely to indicate this fact.

§ To whom correspondence should be addressed: Harvard Institutes of Medicine, 77 Ave. Louis Pasteur, Boston, MA 02115. Tel.: 617-525-5200; Fax: 617-525-5252; E-mail: DSelkoe@cnd.bwh.harvard.edu.

[1] The abbreviations used are: Aβ, amyloid β-protein; AD, Alzheimer's disease; IDE, insulin-degrading enzyme; HPLC, high pressure liquid chromatography; FAβB, fluorescein-Aβ-(1–40)-Lys-biotin; FP, fluorescence polarization; NEP, neprilysin; Bis-Tris, 2-[bis(2-hydroxyethyl) amino]-2-(hydroxymethyl)propane-1,3-diol; AP, avidin-agarose precipitation.

half to one-third of the concentration calculated from lyophilized peptide weight.

Proteases—The cDNA for human IDE beginning with the translation start site at Met^{42} was subcloned into the pFastBacHT vector (Invitrogen), which codes for an amino-terminal tag containing a His_6 affinity tag followed by a tobacco etch virus protease cleavage site. Baculovirus production and protein expression in Sf9 moth cells were performed at the Wistar Institute (University of Pennsylvania). Recombinant IDE protein was then purified from snap-frozen Sf9 cell pellets by cobalt metal affinity chromatography according to the manufacturer's recommendations (Clontech), and the affinity tag was removed by treatment with tobacco etch virus protease (1000 units/mg of recombinant protein) for 2 h at 22 °C (Invitrogen). The His_6-containing tag and any residual tagged protein were separated from the cleaved IDE by cobalt affinity chromatography, followed by overnight dialysis against two changes of 20 mM KH_2PO_4, pH 7.3, using a dialysis container with a 35-kDa molecular mass cut-off (Millipore). Finally, to separate full-length ~113-kDa recombinant IDE from a prominent ~70-kDa truncated species, the sample was washed and concentrated using a 100-kDa molecular mass cut-off centrifugal filter column (Amicon). Recombinant IDE was stored in aliquots in 100 mM KH_2PO_4, pH 7.3, plus 20% glycerol at −80 °C until further use. Recombinant rabbit secreted NEP (sNEP) produced in *P. Pastoris* (12) was a gift from Drs. Guy Boileau and Philippe Crine (University of Montreal). Human plasmin was purchased from Calbiochem/Novabiochem. Prior to initiation of quantitative studies, optimal conditions for each protease were determined by testing its activity in various buffers (*e.g.* HEPES, Tris-HCl, Bis-Tris-propane, KH_2PO_4) containing either no salt or 100 mM NaCl and prepared at the pH optimum listed in the BRENDA enzyme data base (pH ~7.4 in all cases). All proteases performed optimally in 50 mM HEPES, 100 mM NaCl, 0.05% bovine serum albumin, pH 7.4 (Buffer A); thus, these conditions were used for all subsequent degradation assays.

Liquid Chromatography/Mass Spectrometry—Reverse phase high performance liquid chromatography was done on a Vydac diphenyl column (5 μm; 1 × 150 mm; Hesperia, CA), using a linear gradient (20–80%) of acetonitrile in 0.1% trifluoroacetic acid over 60 min. All components were monitored by UV and visible light absorbance using a Surveyor PDA (three channel outputs at 214, 259, and 495 nm) with a scan rate of 1 Hz and scan step of 1 nm. A nanospray ion source with a 100-μm inner diameter-fused silica capillary was used to introduce the column effluent into an LCQDeca Mass Spectrometer, analyzed in a positive ion mode with a scan range of 200–2500 atomic mass units, using the following source conditions: capillary temperature, 250 °C; spray voltage, 4.56 kV; capillary voltage, 46.11 V; sheath gas, 86.96 (arbitrary units); auxiliary gas, 2.68 (arbitrary units).

FAβB Degradation Assay Using Avidin-Agarose Precipitation (AP)—For progress curves and dose-response experiments, each protease (1–400 nM final concentration) was dissolved in 0.5 ml of Buffer A in 0.65-ml siliconized microcentrifuge tubes (Costar), and the reaction was initiated by adding 100 μl of 6 μM FAβB. For kinetic determinations, different concentrations of FAβB (0.25–150 μM final concentration) were dissolved in 0.5 ml of Buffer A, and the reaction was initiated by adding 100 μl of diluted protease. At various time points (0, 5, and 10 min), 80 μl of the reaction mixture was removed and quenched in 0.72 ml of Buffer A supplemented with the appropriate protease inhibitor (2 mM 1,10-phenanthroline for IDE and NEP or 1 mM phenylmethylsulfonyl fluoride for plasmin). Uncleaved FAβB substrate was precipitated from each quenched reaction by the addition of suitable quantities of Neutravidin™-coated agarose beads (Pierce) followed by gentle rocking for 30 min and centrifugation at 14,000 × *g* for 10 min. The supernatant (containing cleaved fluorescein-Aβ fragments) was carefully transferred in three 200-μl aliquots to black 96-well plates (Nunc), and fluorescence intensity (488 excitation, 515 emission) was measured using a Victor2 multilabel plate reader (PerkinElmer Life Sciences). All AP assays were performed at 37 °C. Activity was normalized to control reactions containing either no protease or excess protease. Quantitative kinetic data were derived by hyperbolic regression analysis using the computer program HYPER.EXE created by John S. Easterby (University of Liverpool).

FAβB Degradation Assays Using FP—FP degradation assays carried out at 37 °C were performed as above, except that 30-μl aliquots were quenched in 170 μl of Buffer A supplemented with 1 μM egg white avidin (Molecular Probes, Inc., Eugene, OR) plus appropriate protease inhibitor(s). After incubating at room temperature for 15 min, quenched reactions were loaded in quadruplicate onto "nonbinding surface" 384-well plates (Corning), and fluorescence polarization (excitation, 488; emission, 515) was determined using a Victor2 multilabel plate reader (PerkinElmer Life Sciences).

Robot-assisted, High Throughput FP FAβB Degradation Assays—High throughput experiments were conducted on a customized apparatus (SAGIAN; Beckman) containing a 3-meter rail ORCA robot that integrates a Biomek FX liquid handling station, a SAGIAN core system, and SAGIAN six-plate shaker. Recombinant IDE (0.3–3 nM final concentration) dissolved in Buffer A (20 μl/well) was loaded onto "nonbinding surface" 384-well plates (Corning). Following a 20-min incubation period at room temperature, FAβB (1 μM) in Buffer A (20 μl/well) was added to initiate the reactions. Reactions were terminated with 10 μl/well Buffer A supplemented with 10 mM 1,10-phenanthroline and 5 μM avidin. FP values were determined on an LJL Analyst HT (488-nm excitation, 515-nm emission).

Performance of the assay in the high throughput format was evaluated by computing the *Z*-factor values (13) according to the following formula,

$$Z = 1 - \frac{(3 * (\sigma_{HI} + \sigma_{LO}))}{\bar{X}_{HI} - \bar{X}_{LO}} \quad \text{(Eq. 1)}$$

where σ_{HI} and σ_{LO} designate the S.D. values and $\bar{X}_{HI}$ and $\bar{X}_{LO}$ represent the means of data from internal controls representing 100 and 0% activity, respectively. Using this formula, an ideal assay would have a Z-factor value approaching 1.0, and assays with values below ~0.5 would generally be considered unreliable.

Inhibitor Profiles Determined in Rat Brain Membrane Fractions Using FAβB FP Versus ^{125}I-Aβ-(1–40)-Trichloroacetic Acid Precipitation Assays—Fresh-frozen rat cerebral hemispheres were homogenized in 8 volumes (w/v) of 0.25 M sucrose in 50 mM Tris-HCl (pH 7.4) in a Potter-Elvehjem homogenizer. After pelleting nuclei and unbroken cells, the supernatant was spun again at 100,000 × *g* for 1 h. This resulting supernatant was saved as the soluble fraction, and the membrane pellet was washed in 100 mM Na_2CO_3 (pH 11.3) to linearize microsomes and strip adventitiously associated proteins (14). The membranes were pelleted by another 1-h spin at 100,000 × *g*, resuspended in 50 mM Tris-HCl (pH 7.4), and sonicated by a 10-s pulse with a model 300 sonic dismembrator (Fisher) set at 60% maximum power. Protein concentrations were determined using a bicinchoninic acid-based protein assay (Pierce). For trichloroacetic acid precipitation-based Aβ degradation assays, 100 pM synthetic human ^{125}I-Aβ-(1–40) (Amersham Biosciences) was incubated at 37 °C with 100 μg/ml membrane fractions in 50 mM Tris-HCl (pH 7.4) with or without various inhibitors. At various time points (*e.g.* 3 and 6 h), an aliquot of the sample was added to an equal volume of 15% trichloroacetic acid to precipitate uncleaved peptides. Following centrifugation, radioactivity in the trichloroacetic acid-insoluble pellet (undegraded peptide) and trichloroacetic acid supernatant (degraded peptide fragments) were determined, and the percentage of radiolabeled substrate degraded was calculated. The FP assay was performed as described above using identical quantities of the same brain membranes. Recombinant insulin, purified glucagon, thiorphan, and 1,10-phenanthroline were from Sigma.

RESULTS

FAβB and Wild-type Aβ Are Cleaved at Similar Sites by IDE and NEP—To identify the cleavage sites of wild-type and derivatized Aβ peptides, aliquots of each peptide (10–50 μM final concentration) were digested with IDE or NEP for various lengths of time at 37 °C, and the resulting peptide fragments were analyzed by liquid chromatography/mass spectrometry. Consistent with previous reports (15–17), wild-type Aβ-(1–40) was hydrolyzed by IDE primarily at the Val^{13}-His^{14}, His^{14}-His^{15}, His^{15}-Gln^{16}, Phe^{19}-Phe^{20}, Phe^{20}-Ala^{21}, and Lys^{28}-Gly^{29} peptide bonds, and FAβB was hydrolyzed at identical sites (Fig. 1*A* and Table I). The major peptide fragments detected immediately following IDE hydrolysis were, in order of abundance, Asp^1-His^{14}, Asp^1-His^{13}, Asp^1-Lys^{28}, Asp^1-Phe^{19}, and Phe^{20}-Val^{40}. Upon incubation with NEP, both wild-type Aβ-(1–40) and FAβB were cleaved predominantly at identical peptide bonds, including several detected previously (Glu^9-Tyr^{10}, Phe^{19}-Phe^{20}, Ala^{30}-Ile^{31}, and Glu^{33}-Leu^{34}) (18) as well as others not previously reported (*e.g.* Ala^2-Glu^3, His^{13}-His^{14}) (Fig. 1*B* and Table II). The initial peptide fragments detected, in order of abundance, were Phe^{20}-Ala^{30}, Phe^{20}-Lys^{28}, Phe^{20}-Gly^{29}, and His^{14}-Gly^{25}.

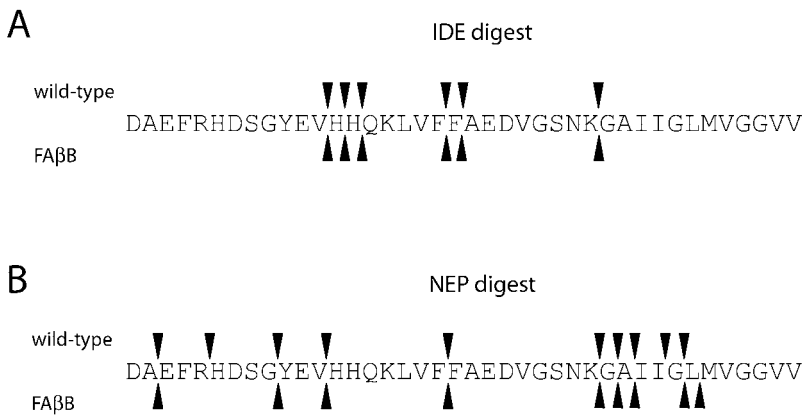

FIG. 1. **Fluorescein-Aβ-(1–40)-Lys-biotin (FAβB) is cleaved at similar sites as wild-type Aβ-(1–40).** Amino acid sequence of Aβ-(1–40) depicting scissile bonds of FAβB (*upper arrowheads*) and wild-type Aβ-(1–40) (*lower arrowheads*) cleaved by IDE (*A*) or NEP (*B*), as determined by liquid chromatography/mass spectroscopy, is shown. The proteolytic fragments identified by liquid chromatography/mass spectrometry are listed in Tables I and II.

TABLE I
Proteolytic fragments of wild-type Aβ and FAβB detected by liquid chromatography/mass spectrometry following digestion with IDE
Mass values are shown in atomic mass units.

IDE digest Aβ fragment	Wild type Aβ-(1–40)		FAβB	
	Expected mass	Observed mass	Expected mass	Observed mass
1–13	1561.6	1562.5	1919.6	1921.0
1–14	1699.6	1699.6	2057.6	2058.6
1–15	1827.9	1829.0	2184.9	2184.0
1–19	2314.5	2314.8	2672.5	2671.4
1–20	2461.9	2462.3	2818.9	NF
1–21	2532.8	2533.6	2890.0	NF
14–28	1719.3	1719.9	1719.3	1719.9
15–28	1582.2	1582.8	1582.2	1582.8
15–40	2649.1	2651.2	3090.4	3090.2
16–21	724.2	724.9	724.2	NF
16–40	2486.0	2487.0	2980.0	2980.0
20–28	966.8	NF	966.8	967.0
21–40	1886.2	1886.9	2327.4	2328.2
22–40	1814.9	NF	2256.0	2256.9
1–40	4330.6	4329.9	5616.0	5155.8
1–40(OX)	4345.9	4346.1	5172.0	5171.4

TABLE II
Proteolytic fragments of wild-type Aβ and FAβB detected by liquid chromatography/mass spectrometry following digestion with NEP
Values are shown in atomic mass units.

NEP digest Aβ fragment	Wild type Aβ-(1–40)		FAβB	
	Expected mass	Observed mass	Expected mass	Observed mass
1–13	1561.6	1562.5	1919.6	1921.0
3–9	847.9	NF	847.9	849.0
3–19	2129.3	2129.2	2129.3	NF
6–9	415.4	414.5	415.4	NF
14–30	1848.1	1849.2	1848.1	NF
14–32	2074.4	2074.3	2074.4	NF
14–33	2131.4	2131.2	2131.4	2132.5
14–34	2244.6	NF	2244.6	2244.3
20–28	967.0	966.7	967.0	966.7
20–29	1024.1	1023.9	1024.1	1023.6
20–30	1095.2	1094.7	1095.2	1094.7
30–33	373.5	372.5	373.5	NF
31–33	302.4	NF	302.4	301.8
31–40	957.2	NF	1398.3	1397.2
1–40	4330.6	4332.2	5616.0	5155.8
1–40(OX)	4345.9	4346.1	5172.0	5171.4

Measurement of FAβB Proteolysis by Fluorescence Polarization—FP is a sensitive method for measuring the relative mass of fluorescent molecules in solution (19). Stationary fluorescent molecules, when excited with plane-polarized light, emit photons polarized in the same plane as (or at a fixed angle to) the light used for excitation. Fluorescent molecules in solution, by contrast, rotate (or tumble) at a rate that is inversely proportional to their mass. Because there is an appreciable time delay between absorption and emission of photons by the fluorescent molecule, tumbling causes emitted light to be depolarized relative to the plane-polarized light used for excitation. The degree of depolarization (reflecting the average mass of all fluoresceinated species) can be quantified accurately using appropriately equipped fluorometers.

To effectively measure proteolysis using FP, there must be a substantial mass difference between the intact, fluorescently tagged substrate and the cleaved, fluorescently tagged proteolytic fragments. The addition of a biotin moiety at the opposite end of the molecule to the fluorescent tag allows the molecular weight of the intact substrate to be increased (to ~70 kDa) by adding excess avidin at the end of the reaction. The molecular weights of the cleaved, fluoresceinated NH_2-terminal fragments (<4 kDa), by contrast, remain unaffected by the presence of avidin and tumble rapidly. The relative amounts of cleaved and uncleaved substrate can then be accurately measured using FP. The robust and reproducible nature of our FP-based FAβB degradation assay is illustrated in Fig. 2*A*, which shows progress curves with very small S.D. values for the degradation of FAβB by IDE or by NEP.

Because of concern about the tendency of Aβ peptides to aggregate and/or adsorb nonspecifically to the surfaces of reaction vessels, we also tested a version of the derivatized substrate lacking the hydrophobic carboxyl-terminal 12 amino acids (*i.e.* fluorescein-Aβ-(1–28)-biotin). However, this species proved to be a relatively poor substrate for IDE and other Aβ-degrading proteases (data not shown) and was not pursued further. We were able to overcome adsorption problems associated with full-length FAβB substrate by adding 0.05% bovine serum albumin to the assay buffer and by keeping the substrate concentration above 20 nM (see below).

Measurement of FAβB Proteolysis by Avidin-Agarose Precipitation—The FAβB substrate can be incorporated into another fluorescence-based degradation assay we developed that does not require the specialized equipment used to measure FP. In this assay, avidin-conjugated agarose beads are used to centrifugally separate uncleaved FAβB from the fluoresceinated (nonbiotinylated) amino-terminal proteolytic fragments; the amount of fluorescence remaining in the supernatant corresponds directly to the amount of proteolysis. As shown in Fig. 2*B*, this AP method yielded virtually identical results to the FP-based method in parallel experiments (*cf.* Fig. 2, *A* and *B*; see also Fig. 4, *A* and *B*). Whereas the AP assay has the advantage of requiring no specialized equipment, the requirement for a centrifugation step precludes its use in high throughput compound screening; consequently, our further work focused on the validation and miniaturization of the FP assay.

Specificity of the FAβB Substrate in Biological Samples—To test the FP FAβB degradation assay with biological material,

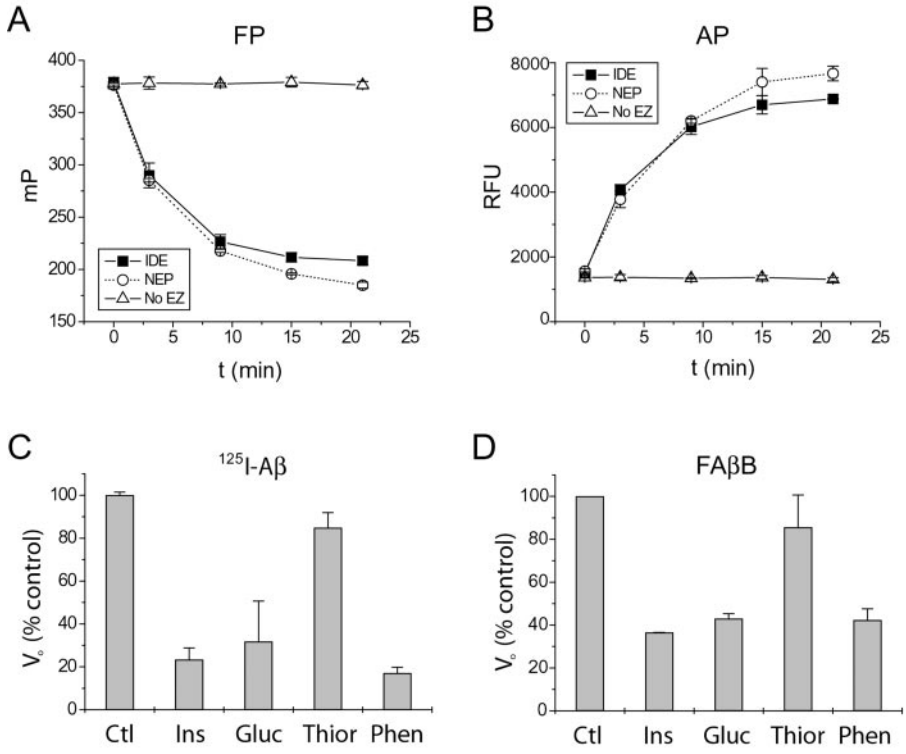

FIG. 2. **Proteolysis of FAβB by recombinant and brain-derived proteases.** Progress curves for hydrolysis of FAβB (1 μM) by IDE (5 nM) and NEP (150 nM) using the FP (*A*) and the AP (*B*) *in vitro* degradation assays are shown. ^{125}I-Aβ-(1–40) (*C*) and FAβB (*D*) degradation assays show closely similar inhibitor profiles following incubation with bicarbonate-washed rat brain membranes. The *bars* are means ± S.D. for 3–8 replications. *Ctl*, no inhibitor; *Ins*, insulin (10 μM); *Gluc*, glucagon (10 μM); *Thior*, thiorphan (2 mM); *Phen*, 1,10-phenanthroline (2 mM).

we determined the inhibition profile of FAβB using bicarbonate-washed rat brain membrane fractions, which contain a wide array of proteases, and compared the result with that determined using a standard ^{125}I-Aβ-(1–40)/trichloroacetic acid precipitation assay (4, 20). As we have recently reported elsewhere (4), the majority of ^{125}I-Aβ-(1–40) degradation in membrane fractions is competitively inhibited by insulin or glucagon, which are avid IDE substrates, whereas a smaller fraction is inhibited by thiorphan, which is a potent inhibitor of NEP (Fig. 2*C*). 1,10-Phenanthroline, a broad spectrum inhibitor of zinc-metalloproteases, also strongly inhibited ^{125}I-Aβ-(1–40) degradation, as expected. Hydrolysis of FAβB, determined in the same biological samples using the FP assay, exhibited a highly similar inhibition profile (Fig. 2*D*). Thus, FAβB is an avid substrate for multiple known Aβ-degrading proteases and is suitable for *in vitro* degradation assays on biological samples.

Validation of the FP Assay—To directly test the linearity of the FP assay, we determined the polarization values produced by aliquots of FAβB (1 μM) containing predetermined percentages of uncleaved substrate and substrate previously digested with IDE or NEP. As shown in Fig. 3*A*, the change in polarization values, normalized to the maximum obtained with each protease, varied in a nearly linear fashion with percentage of hydrolyzed substrate. Because quantitative assays depend on accurate determinations of the initial velocities of substrate hydrolysis, which are typically determined from the first 10–20% of a progress curve, we quantified the deviation from linearity observed in this range. The FP assay was found to overestimate the initial velocity by ~10% for hydrolysis by either protease (Fig. 3*A*). Hence, this figure was used as a correction factor in subsequent quantitative determinations (Fig. 4*A*).

During the development of the FP assay, we initially sought to maintain a low (5–20 nM) substrate concentration before reading the polarization values, since such levels are typically used for FP applications. This constraint precluded attempts to miniaturize the assay for high throughput screening, because proteolysis was inefficient and highly variable at such low substrate concentrations and because protocols involving further dilution of the substrate were undesirable. However, additional testing revealed that the FP assay was actually most linear, in terms of absolute polarization values, in the range of substrate concentrations between 100 and 1000 nM (Fig. 3*B*). The working range could be extended further, provided the resultant data were normalized to empirically determined maximal and minimal polarization values at each substrate concentration (see below), and in practice, such normalization was routinely used. This range of suitable substrate concentrations in the FP assay had several practical benefits, particularly for kinetic analyses requiring variable concentrations of substrate.

High Throughput FP Degradation Assay—To test the performance of the FP assay in a high throughput, robot-assisted format, various concentrations of recombinant IDE (0.3–3 nM final concentration) were transferred robotically to 384-well plates containing 0.2 μl of Me_2SO (0.5% final concentration). The reactions were initiated by adding FAβB (0.5 μM final concentration) and terminated at various times by the addition of assay buffer containing 1,10-phenanthroline and avidin. The assay performed superiorly in this format (Fig. 3*C*), routinely yielding *Z*-factor values greater than 0.8 (see "Materials and Methods").

Kinetic Analysis of FAβB Degradation by IDE, NEP, and Plasmin—The AP and FP assays were used to obtain quantitative kinetic data for three different Aβ-degrading proteases: IDE, NEP, and plasmin. Data for endothelin-converting enzyme-1 and -2 were not determined due to lack of availability of the purified enzyme. Because even freshly dissolved Aβ peptides consist of unknown fractions of oligomerized species, we were careful to first remove aggregated FAβB peptides by high speed centrifugation and then quantify the absolute concentration of peptide by amino acid analysis (see "Materials and Methods"). Lineweaver-Burk plots of these kinetic determinations are illustrated in Fig. 4, *A–C*, whereas quantitative data derived by hyperbolic regression analysis of the raw data are provided in Table III. For each

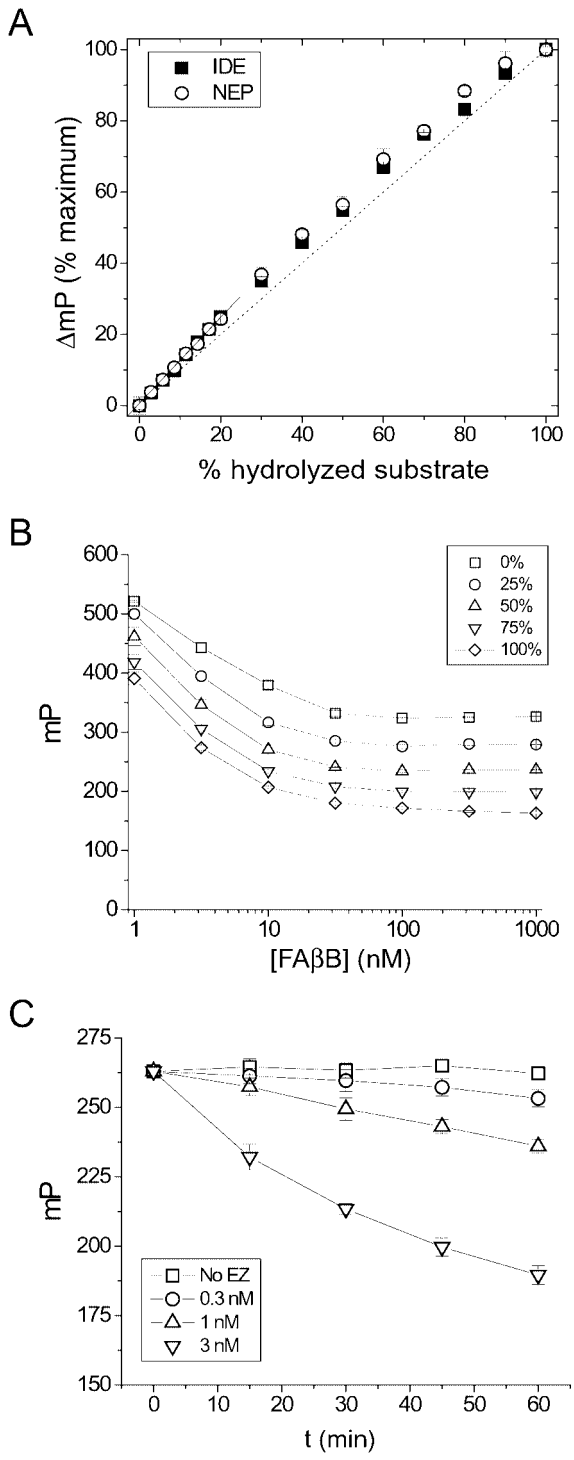

FIG. 3. **Validation of the FP degradation assay.** The FP degradation assay yields nearly linear quantitative data across a broad range of substrate concentrations. *A*, percentage change in polarization values (ordinate) plotted as a function of the percentage of hydrolyzed substrate (*abscissa*) using the enzymes IDE (■) or NEP (○). The *solid line* depicts the slight deviations from perfect linearity (*dashed line*) in the slope of FP data between 0 and 20% hydrolyzed substrate. *B*, absolute polarization values (*mP*) plotted as a function of substrate concentration (nM). Data from different percentages of hydrolyzed substrate are shown. *C*, progress curves of FAβB hydrolysis by increasing concentrations of recombinant IDE determined using the FP assay in a high throughput (384-well) robotic format. *mP*, millipolarization units.

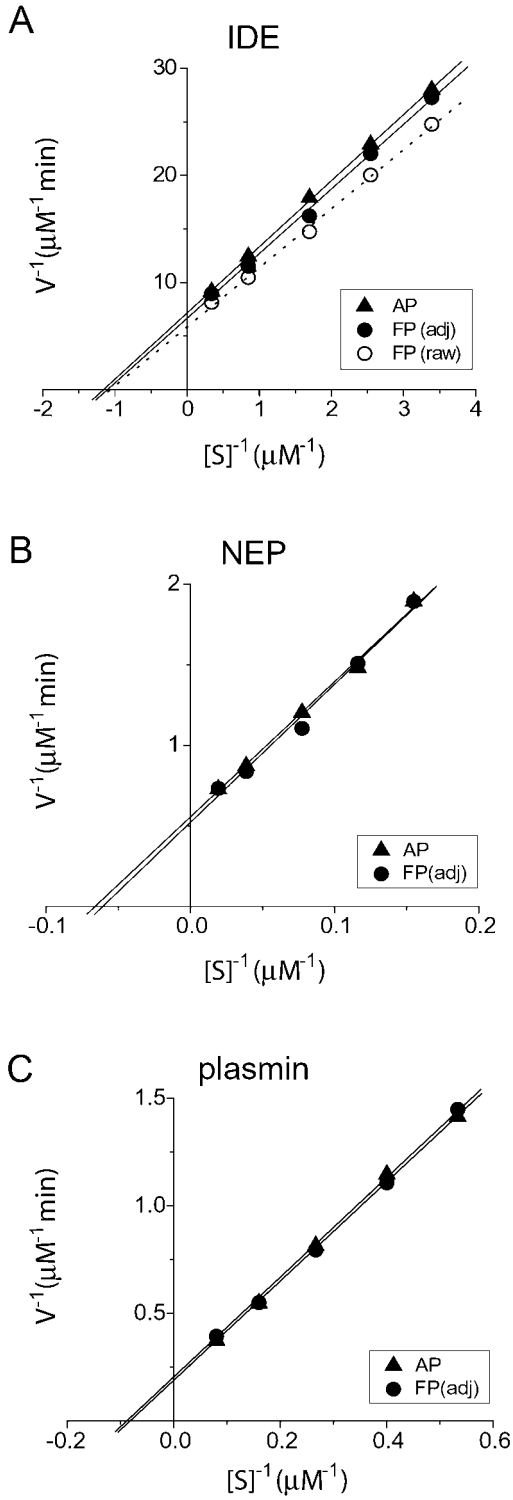

FIG. 4. **Kinetic analysis of FAβB degradation.** Lineweaver-Burk plots of FAβB hydrolyzed by IDE (*A*), NEP (*B*), and plasmin (*C*). Data were determined by FP (●) and AP (▲) degradation assays. *Open circles* in *A* represent FP data before correction for minor nonlinearity in FP progress curves (see Fig. 3*A*). Kinetic parameters, determined by hyperbolic regression analysis, are given in Table III.

protease, very similar quantitative kinetic data were obtained with the AP and the FP assays, and the data were in even closer agreement after correcting for the slight overestimation in initial velocity that occurs with the FP assay (see above and Figs. 3*A* and 4*A*).

Applications of the FAβB Degradation Assays—To highlight the utility of the FP assay in generating highly reliable quantitative data, we performed several demonstration experiments using medium throughput protocols optimized for 96-well plates. Fig. 5*A* shows raw progress curves from a typical ex-

TABLE III
Kinetic parameters of FAβB degradation by Aβ-degrading proteases

	IDE		NEP		Plasmin	
	FP[a]	AP	FP[a]	AP	FP[a]	AP
k_m (μM)	0.82 ± 0.06	0.87 ± 0.10	13.5 ± 1.2	14.4 ± 1.2	12.1 ± 1.8	10.9 ± 1.4
v_{max} (μM min^{-1})	0.17 ± 0.01	0.16 ± 0.01	1.76 ± 0.12	1.77 ± 0.11	5.89 ± 0.53	4.71 ± 0.36
k_{cat} (min^{-1})	256 ± 22	221 ± 11	88 ± 6	89 ± 6	118 ± 11	94 ± 7
k_{cat}/k_m (M^{-1} min^{-1})	3.1×10^8	2.5×10^8	6.5×10^6	6.2×10^6	9.8×10^6	8.6×10^6

[a] Data calculated using correction factor derived from Fig. 3*A*.

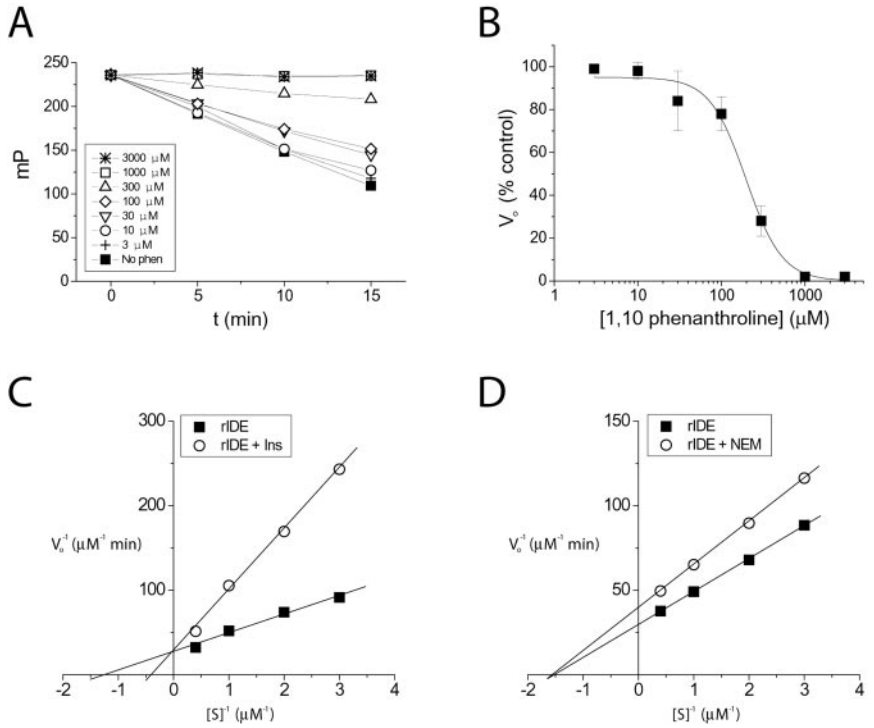

FIG. 5. **Quantitative applications of the FAβB degradation assay.** *A*, typical progress curves in an experiment determining the IC_{50} of 1,10-phenanthroline on IDE-mediated hydrolysis of FAβB. *B*, the average of three experiments such as that shown in *A*. *C*, Lineweaver-Burk plots of kinetic data for the hydrolysis of FAβB by IDE without (■) or with (○) insulin (100 nM), an avid competitive substrate. *D*, Lineweaver-Burk plots of kinetic data for inhibition by *N*-ethylmaleimide (30 μM), an irreversible, noncompetitive inhibitor.

periment that determined the IC_{50} for inhibition of IDE-mediated FAβB degradation by 1,10-phenanthroline. The dose-response relationship, determined from the average of three such experiments, is illustrated in Fig. 5*B*. Fig. 5*C* shows Lineweaver-Burk plots for inhibition of FAβB degradation by insulin, an avid substrate of IDE. Note that these results are characteristic of competitive inhibition, as expected. For comparison, Fig. 5*D* shows comparable data for inhibition by *N*-ethylmaleimide, an irreversible thiol-alkylating agent, and this experiment yielded the expected profile for a noncompetitive inhibitor. Collectively, these experiments show that the FP FAβB degradation assay is highly quantitative, reproducible, and capable of revealing insights into the detailed kinetics of Aβ-degrading proteases.

DISCUSSION

Evidence emerging from numerous laboratories has highlighted the importance of Aβ-degrading proteases in regulating steady-state cerebral Aβ levels *in vivo* (2–5). Inherited defects in one or more of these proteases could explain Aβ accumulation in some cases of AD, but regardless of whether such genetic connections are found, these enzymes provide potentially attractive drug targets for treating all cases of the disease. However, traditional methods for studying Aβ degradation (*e.g.* trichloroacetic acid precipitation assays with iodinated Aβ, HPLC analysis of synthetic radiolabeled or unlabeled Aβ, and autoradiography of metabolically labeled Aβ) are ill suited for high throughput compound screening or routine quantitative assays. To meet this important need, we have developed and characterized versatile and quantitative assays that utilize the derivatized Aβ peptide, FAβB.

Several lines of evidence indicate that degradation of FAβB is similar to that of wild-type Aβ. First, the derivatized peptide is avidly degraded by several different proteases that have been shown to degrade Aβ: IDE, NEP, and plasmin. Second, liquid chromatography/mass spectrometric analysis shows that wild-type and derivatized Aβ are cleaved at nearly identical sites by IDE and NEP, the two most extensively characterized Aβ-degrading proteases. Third, degradation of FAβB and ^{125}I-Aβ-(1–40) show closely similar inhibition profiles when incubated in biological samples containing an array of competing proteases. These findings suggest that the fluorescein and lysine-biotin moieties do not significantly alter the cleavage specificity of the substrates by the Aβ-degrading proteases investigated here.

Additional support for the validity of our FAβB substrate comes from analysis of quantitative data from kinetic determinations. Independent analyses using the FP- and AP-based assays yielded quantitatively similar estimates of kinetic parameters for hydrolysis, and this pertained for all three Aβ-degrading proteases. Moreover, kinetic determinations using FAβB (Table I) yielded absolute quantitative data that are in good agreement with published values using wild-type synthetic Aβ. For instance, apparent k_m values of ~2 μM have been reported for degradation of wild-type Aβ-(1–40) in independent studies utilizing purified (21) or recombinant (22) human IDE. By comparison, the apparent k_m values obtained using our FP and AP assays were 0.82 and 0.87 μM, respectively. Whereas

these values are lower than the published values, this discrepancy disappears after it is noted that about one-half to two-thirds of the lyophilized peptide was pelleted by high speed centrifugation and thus in an aggregated state that is incapable of degradation by IDE (see Ref. 23). Indeed, when freshly dissolved substrate was used, we obtained kinetic parameters that closely matched the published values for IDE ($k_m = 2.11 \pm 0.20$ μM). These results suggest that caution should be exercised in interpreting kinetic data for Aβ degradation when the peptide's aggregation state has not been characterized.

Our liquid chromatography/mass spectrometric analysis revealed that NEP-mediated hydrolysis of Aβ (both wild-type and derivatized) occurred at substantially more sites than previously reported by Howell *et al.* (18), with considerable heterogeneity observed at the carboxyl terminus of the peptide (Fig. 1*B*). This discrepancy may be explained by the fact that the latter study focused only on the initial peptide fragments detectable upon hydrolysis with NEP. However, it is also possible that our analysis was more sensitive, given the fact that the LC and MS analyses were coupled within the same instrument. Relative to IDE, it appears that NEP shows less cleavage specificity within Aβ. In addition, the k_m for hydrolysis of FAβB by NEP (~14 μM) is more than 17 times larger than that for IDE (~0.8 μM; see Table I). We note that comparison with reported k_m values for Aβ hydrolysis by NEP is complicated by the fact that we used a secreted form of rabbit NEP, whereas published values for wild-type Aβ degradation were determined using membrane-anchored NEP (24). However, the secreted NEP used in this study has been directly compared with membrane-anchored NEP, and found to exhibit similar kinetics parameters using the preferred substrate, [D-Ala^2,D-Leu^5]enkephalin (12). To our knowledge, the k_m value for Aβ degradation by plasmin has not been determined previously.

In conclusion, we have developed sensitive and quantitative assays for the study of the proteolytic degradation of Aβ. The assays are simple, highly reproducible, inexpensive, and suitable for high throughput screening. Implementation of these assays should yield novel insights into the detailed kinetics of various Aβ-degrading proteases and facilitate the identification of novel small molecule pharmacophores.

Acknowledgments—We thank Drs. Guy Boileau and Philippe Crine for the soluble NEP, Alice Y. Chang for assistance with purification of recombinant IDE, and Dr. Li-An Yeh and Jake Ni for assistance with robotic screening.

REFERENCES

1. Selkoe, D. (2001) *Neuron* **32,** 177–180
2. Iwata, N., Tsubuki, S., Takaki, Y., Shirotani, K., Lu, B., Gerard, N. P., Gerard, C., Hama, E., Lee, H. J., and Saido, T. C. (2001) *Science* **292,** 1550–1552
3. Eckman, E. A., Watson, M., Marlow, L., Sambamurti, K., and Eckman, C. B. (2003) *J. Biol. Chem.* **278,** 2081–2084
4. Farris, W., Mansourian, S., Chang, Y., Lindsley, L., Eckman, E. A., Frosch, M. P., Eckman, C. B., Tanzi, R. E., Selkoe, D. J., and Guenette, S. (2003) *Proc. Natl. Acad. Sci. U. S. A.* **100,** 4162–4167
5. Miller, B. C., Eckman, E. A., Sambamurti, K., Dobbs, N., Chow, K. M., Eckman, C. B., Hersh, L. B., and Thiele, D. L. (2003) *Proc. Natl. Acad. Sci. U. S. A.* **100,** 6221–6226
6. Bertram, L., Blacker, D., Mullin, K., Keeney, D., Jones, J., Basu, S., Yhu, S., McInnis, M. G., Go, R. C., Vekrellis, K., Selkoe, D. J., Saunders, A. J., and Tanzi, R. E. (2000) *Science* **290,** 2302–2303
7. Li, Y. J., Scott, W. K., Hedges, D. J., Zhang, F., Gaskell, P. C., Nance, M. A., Watts, R. L., Hubble, J. P., Koller, W. C., Pahwa, R., Stern, M. B., Hiner, B. C., Jankovic, J., Allen, F. A., Jr., Goetz, C. G., Mastaglia, F., Stajich, J. M., Gibson, R. A., Middleton, L. T., Saunders, A. M., Scott, B. L., Small, G. W., Nicodemus, K. K., Reed, A. D., Schmechel, D. E., Welsh-Bohmer, K. A., Conneally, P. M., Roses, A. D., Gilbert, J. R., Vance, J. M., Haines, J. L., and Pericak-Vance, M. A. (2002) *Am. J. Hum. Genet.* **70,** 985–993
8. Ait-Ghezala, G., Abdullah, L., Crescentini, R., Crawford, F., Town, T., Singh, S., Richards, D., Duara, R., and Mullan, M. (2002) *Neurosci. Lett.* **325,** 87–90
9. Ermolieff, J., Loy, J. A., Koelsch, G., and Tang, J. (2000) *Biochemistry* **39,** 16263
10. Kimberly, W. T., Esler, W. P., Ye, W., Ostaszewski, B. L., Gao, J., Diehl, T., Selkoe, D. J., and Wolfe, M. S. (2003) *Biochemistry* **42,** 137–144
11. Karlstrom, H., Bergman, A., Lendahl, U., Naslund, J., and Lundkvist, J. (2002) *J. Biol. Chem.* **277,** 6763–6766
12. Beaulieu, H., Elagoz, A., Crine, P., and Rokeach, L. A. (1999) *Biochem. J.* **340,** 813–819
13. Zhang, J. H., Chung, T. D., and Oldenburg, K. R. (1999) *J. Biomol. Screen.* **4,** 67–73
14. Fujiki, Y., Hubbard, A. L., Fowler, S., and Lazarow, P. B. (1982) *J. Cell Biol.* **93,** 97–102
15. Mukherjee, A., Song, E., Kihiko-Ehmann, M., Goodman, J. P., Jr., Pyrek, J. S., Estus, S., and Hersh, L. B. (2000) *J. Neurosci.* **20,** 8745–8749
16. Chesneau, V., Vekrellis, K., Rosner, M. R., and Selkoe, D. J. (2000) *Biochem. J.* **351,** 509–516
17. Morelli, L., Llovera, R., Gonzalez, S. A., Affranchino, J. L., Prelli, F., Frangione, B., Ghiso, J., and Castano, E. M. (2003) *J. Biol. Chem.* **278,** 23221–23226
18. Howell, S., Nalbantoglu, J., and Crine, P. (1995) *Peptides* **16,** 647–652
19. Jameson, D. M., and Sawyer, W. H. (1995) *Methods Enzymol.* **246,** 283–300
20. Vekrellis, K., Ye, Z., Qiu, W. Q., Walsh, D., Hartley, D., Chesneau, V., Rosner, M. R., and Selkoe, D. J. (2000) *J. Neurosci.* **20,** 1657–1665
21. Perez, A., Morelli, L., Cresto, J. C., and Castano, E. M. (2000) *Neurochem. Res.* **25,** 247–255
22. Chesneau, V., and Rosner, M. R. (2000) *Protein Expression Purif.* **19,** 91–98
23. Walsh, D. M., Klyubin, I., Fadeeva, J. V., Cullen, W. K., Anwyl, R., Wolfe, M. S., Rowan, M. J., and Selkoe, D. J. (2002) *Nature* **416,** 535–539
24. Shirotani, K., Tsubuki, S., Iwata, N., Takaki, Y., Harigaya, W., Maruyama, K., Kiryu-Seo, S., Kiyama, H., Iwata, H., Tomita, T., Iwatsubo, T., and Saido, T. C. (2001) *J. Biol. Chem.* **276,** 21895–21901